Quasiparticle entropy in superconductor/normal metal/superconductor proximity junctions in the diffusive limit

P. Virtanen,[1,*] F. Vischi,[1,2] E. Strambini,[1] M. Carrega,[1] and F. Giazotto[1]
[1]*NEST, Istituto Nanoscienze-CNR and Scuola Normale Superiore, I-56127 Pisa, Italy*
[2]*Dipartimento di Fisica, Università di Fisica, I-56127 Pisa, Italy*
(Received 11 September 2017; revised manuscript received 31 October 2017; published 26 December 2017)

We discuss the quasiparticle entropy and heat capacity of a dirty superconductor/normal metal/superconductor junction. In the case of short junctions, the inverse proximity effect extending in the superconducting banks plays a crucial role in determining the thermodynamic quantities. In this case, commonly used approximations can violate thermodynamic relations between supercurrent and quasiparticle entropy. We provide analytical and numerical results as a function of different geometrical parameters. Quantitative estimates for the heat capacity can be relevant for the design of caloritronic devices or radiation sensor applications.

DOI: 10.1103/PhysRevB.96.245311

I. INTRODUCTION

Recently a growing interest has been put on the investigation of thermodynamic properties of nanosystems where coherent effects can be both of fundamental interest and useful for applications [1–5]. In particular, superconductor junction systems have attracted interest as they exhibit phase-dependent thermal transport enabling coherent caloritronic devices [3,6–11] and have properties useful for cooling systems in solid-state devices [12–15]. Reciprocally, they enable conversion between thermal currents and electric signals, leading to applications in electronic thermometry [3,16,17], bolometric sensors, and single-photon detectors [18–25]. In such applications, detailed understanding of the thermodynamic aspects of hybrid superconducting/normal metal (SN) structures is crucial, in particular, the interplay between the energy and entropy related to quasiparticles and supercurrents.

The entropy S of noninteracting quasiparticles at equilibrium is determined generally by their density of states (DOS). In the superconducting state, it is modified by the appearance of an energy gap in the spectrum. In extended Josephson junctions, such as superconductor/normal metal/superconductor (SNS) structures, the modification of the DOS depends both on the formation of Andreev bound states inside the junction and the inverse proximity (IP) effect in the superconducting banks, both being modulated by the phase difference φ between the superconducting order parameters [26,27]. Reflecting the fact that the Andreev bound states carry the supercurrent I across the junction, a thermodynamic Maxwell relation,

$$\frac{dS}{d\varphi} = -\frac{\hbar}{2e}\frac{dI}{dT} = -\frac{d^2F}{dT\,d\varphi} \tag{1}$$

connects the entropy and the supercurrent to the temperature T and phase derivative of the free-energy F. The entropy in superconductors can be expressed in terms of the DOS [28] or in terms of Green's functions [29,30]. Moreover, the phase-dependent part of S can be obtained from the current-phase relation (CPR) $I(T,\varphi)$ [26,31] by applying Eq. (1), a contribution important in short junctions [32,33]. The different expressions are mathematically equivalent (see, e.g., Refs. [34,35]). Such equivalences however can be broken by approximations: in particular, the rigid-boundary condition (RBC) approximation [26,31] in which the inverse proximity effect in the superconductors is neglected, invalidates DOS-based expressions for entropy. This approximation predicts successfully many properties of weak-link structures with large superconducting banks compared to the junction region, but as we discuss below, it can be misleading for evaluating thermodynamic quantities of short junctions.

Heat capacity [36–38] and free-energy boundary contributions [35,39–41] in SN systems were considered in several previous works also experimentally [42,43] close to the critical temperature T_c. The inverse proximity effect in the superconducting banks of diffusive SN structures also is studied well [26,31,41,44]. The entropy and heat capacity in diffusive SNS junctions were discussed in Refs. [45,46] but neglecting the inverse proximity effect, which limits the validity of the results to long junctions only.

In this paper, we discuss the proximity effect contributions to the entropy and heat capacity in SNS structures of varying sizes. We also point out reasons for the discrepancies that appear with the RBC approximation in the quasiclassical formalism. We provide analytical results for limiting cases and discuss the crossover regions numerically.

The paper is organized as follows. In Sec. II we introduce the theoretical formalism, based on the Usadel equations and all basic definitions. In Sec. III we discuss the origin of inconsistencies in the RBC approximation. In Sec. IV we present quantitative results for the entropy inside the inverse proximity region and the total entropy. We also show results for the heat capacity in Sec. V and the effect of inverse proximity contributions on this quantity. Section VI concludes with a discussion.

II. THE MODEL AND BASIC DEFINITIONS

Here we consider a Josephson junction as schematically depicted in Fig. 1(a) where two superconducting (S) banks are in clean electric contact with a normal (N) diffusive wire of length L_N. The S and N parts are characterized by cross sections $A_{S,N}$ and electrical conductivities $\sigma_{S,N}$, respectively. Microscopically, the two diffusive regions are characterized

*pauli.virtanen@nano.cnr.it

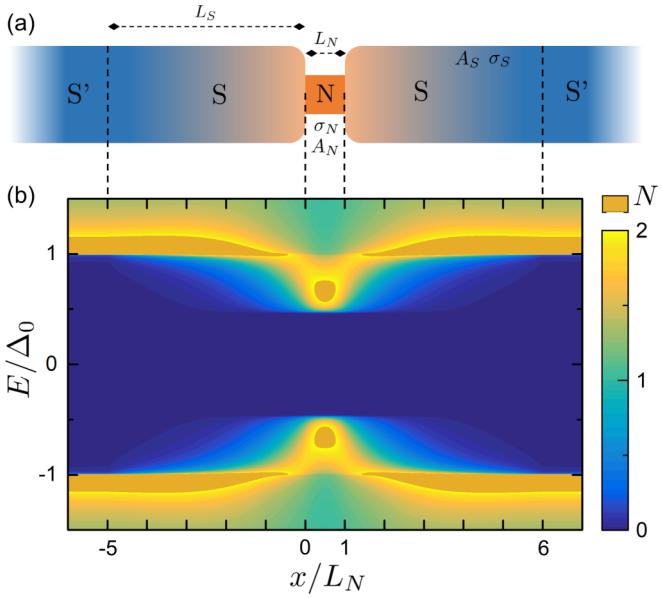

FIG. 1. (a) Schematic of a SNS junction consisting of two superconducting (S) leads in clean electric contact with a normal (N) diffusive nanowire of length L_N. The S and N parts have cross sections $A_{S,N}$ and conductivity $\sigma_{S,N}$. At distances $L_S \gg \xi_S$ from the interface, the properties of the leads approach that of bulk superconductor (S′). (b) Normalized DOS $N(E,x)$ for $\sigma_S A_S/\sigma_N A_N = 1$, $L_N/\xi_N = 1$, and phase difference $\varphi = 0$.

by the diffusion coefficients $D_{S,N}$ and DOS per spin $\mathcal{N}_{0,S}$ and $\mathcal{N}_{0,N}$ at the Fermi level. These quantities are related to conductivities via $\sigma_j = 2e^2 D_j \mathcal{N}_{0,j}$ where the factor 2 takes into account spin degeneracy.

The presence of superconducting leads induces superconducting correlations in the electrons in the normal metal. The correlations at energy E are associated with a characteristic coherence length ξ_E, which in general may differ from the superconducting coherence length $\xi_{N,S} \equiv \sqrt{\hbar D_{N,S}/|\Delta|}$. The superconductors have order parameter Δ with phase difference φ across the junction. We also assume that the superconductor material has critical temperature T_c in bulk.

The entropy density $\mathcal{S}$ and thus the total entropy $S(T,\varphi) = \int dx\, \mathcal{S}(x,T,\varphi)$ can be written in terms of the quasiparticle spectrum,

$$\mathcal{S}(x,T,\varphi) = -4\mathcal{N}_0 \int_{-\infty}^{\infty} dE\, N(E,x,\varphi) f(E,T) \ln f(E,T), \tag{2}$$

where $N(E,x,\varphi)$ is the (reduced) local density of states and $f(E,T) = 1/(e^{E/T}+1)$ is the Fermi distribution function. The normal-state result, without the proximity effect, is found by setting $N(E,x,\varphi) = 1$ in the above expression, giving $\mathcal{S}_n(T) = 2\pi^2 \mathcal{N}_0 T/3$. The entropy density $\mathcal{S}(x,T,\varphi)$ can also be written as

$$\mathcal{S}(x,T,\varphi) = \mathcal{S}_n(x,T) - \frac{d\mathcal{F}_s(x,T,\varphi)}{dT}, \tag{3}$$

where $\mathcal{F}_s = \mathcal{F} - \mathcal{F}_n$ is the difference in the free-energy density between superconducting and normal states.

A functional for the free-energy density difference can be expressed in terms of isotropic quasiclassical Green's functions $\hat{g}$ in the dirty limit [30,47–49],

$$\mathcal{F}_s = \mathcal{N}_0 |\Delta|^2 \ln\frac{T}{T_c} + \pi T \mathcal{N}_0 \sum_{\omega_n} \left[\frac{|\Delta|^2}{\omega_n} + \mathcal{L}(i\omega_n)\right], \tag{4}$$

$$\mathcal{L} = \mathrm{tr}\left\{\omega_n[\mathrm{sgn}(\omega_n) - \tau_3\hat{g}] - (\Delta\tau_+ + \Delta^*\tau_-)\hat{g} + \frac{D}{4}(\hat{\nabla}\hat{g})^2\right\}, \tag{5}$$

where τ_j's indicate Pauli matrices in the Nambu space and $\tau_\pm = (\tau_1 \pm i\tau_2)/2$. The above expression assumes the quasiclassical constraint $\hat{g}^2 = 1$. The long gradient $\hat{\nabla}X = \nabla X - i[\boldsymbol{A}\tau_3, X]$ contains the vector potential $\boldsymbol{A} = (A_x, A_y, A_z)$. The superconducting order parameter is $\Delta = |\Delta| e^{i\phi}$ and $\omega_n = 2\pi T(n+\frac{1}{2})$ are the Matsubara frequencies. The reduced density of states reads $N(E,x,\varphi) = \frac{1}{2}\,\mathrm{Re}\,\mathrm{tr}\,\tau_3\hat{g}(E+i0^+,x,\varphi)$. Here and below, $e = \hbar = k_B = 1$ unless otherwise specified.

The quasiclassical Green's functions can be determined by the Usadel equation [47], which is a Euler-Lagrange equation $\frac{\delta F}{\delta \hat{g}} = 0$ for the free-energy $F = \int dx\, \mathcal{F}$, under the constraint $\hat{g}^2 = 1$. Explicitly we have

$$D\hat{\nabla}\cdot(\hat{g}\hat{\nabla}\hat{g}) - [\omega_n\tau_3 + \Delta\tau_+ + \Delta^*\tau_-, \hat{g}] = 0. \tag{6}$$

The supercurrent I along the x axis at a given position x_0 can be expressed in terms of the above functional as

$$I(x_0) = \frac{\delta F}{\delta A_x(x_0)} = \frac{2e}{\hbar}\frac{dF}{d\varphi}, \tag{7}$$

where φ is an order parameter difference between external leads connected at $x = \pm\infty$. Note that the current generally is conserved only if the order parameter Δ is self-consistent [50], $\delta F/\delta\Delta = \delta F/\delta\Delta^* = 0$ [51]. In non-self-consistent calculations, I is conserved only in the N region where $\Delta(x) = 0$. Below, when we show non-self-consistent results for I, x_0 is in the N region. The second equality in Eq. (7) follows from the gauge transformation

$F[e^{i\chi\tau_3/2}\hat{g}e^{-i\chi\tau_3/2}, \Delta, A_x, \varphi] = F[\hat{g}, \Delta e^{-i\chi}, A_x - \frac{1}{2}\partial_x\chi, \varphi - \chi(\infty) + \chi(-\infty)]$. When computing $I(x_0)$ from a phase derivative of F for non-self-consistent $\Delta(x)$, it is necessary to note that a gauge transform $\partial_x\chi = 2A_x(x)$ eliminating $A_x(x)$ does not only adjust φ, but also adjusts $\Delta \mapsto \Delta e^{-i\chi}$. Below, we take this phase factor into account in phase derivatives so that Eq. (7) also applies in non-self-consistent results.

From Eq. (1) and known current-phase relations [31], the entropy associated with Andreev bound states can also be obtained up to a φ-independent term. From the Kulik-Omel'yanchuk (KO) result [52] for short junctions in the diffusive limit,

$$I(T,\varphi) = \frac{4\pi T}{eR_N}\sum_{\omega_n}\frac{\Delta\cos(\varphi/2)}{\Omega_n}\arctan\frac{\Delta\sin(\varphi/2)}{\Omega_n}, \tag{8}$$

$$S(T,\varphi) - S(T,\varphi=0) = -\frac{\hbar}{2e}\int_0^\varphi d\varphi'\frac{dI}{dT}$$

$$= \frac{\pi\hbar}{2e^2 R_N T^2} \int_{|\Delta||\cos\frac{\varphi}{2}|}^{|\Delta|} dE\, E\, \mathrm{sech}^2\left(\frac{E}{2T}\right) \times \ln \frac{|\Delta|\left|\sin\frac{\varphi}{2}\right| + \sqrt{E^2 - |\Delta|^2\cos^2\frac{\varphi}{2}}}{\sqrt{|\Delta|^2 - E^2}}, \quad (9)$$

where $R_N = L_N/(\sigma_N A_N)$ is the resistance of the normal region and $\Omega_n^2 = \omega_n^2 + |\Delta|^2\cos^2(\varphi/2)$. The temperature dependence of $\Delta(T)$ is ignored, which is valid at low temperatures. The $\varphi = 0$ term can be determined to be $S(\varphi = 0) = 0$ (see below). This result assumes RBC, and including the inverse proximity effect in it would qualitatively result in an increase in L_N by a multiple of the coherence length [26].

For simplicity, in this paper we assume transparent SN interfaces, described by the quasi-one-dimensional (quasi-1D) boundary conditions (e.g., at the left SN contact $x = 0$) [53,54],

$$\hat{g}|_{x\to 0^-} = \hat{g}|_{x\to 0^+}, \quad \sigma_S A_S \hat{g}\,\partial_x\hat{g}|_{x\to 0^-} = \sigma_N A_N \hat{g}\,\partial_x\hat{g}|_{x\to 0^+}, \quad (10)$$

and similarly on the right SN interface at $x = L_N$. The cross-sectional areas appear in the above equations from conservation of the matrix current $\hat{g}\nabla\hat{g}$ [54]; for $A_S \neq A_N$ such a quasi-1D approximation ignores details of the current distribution at the contact, which requires that the cross-sectional size is small compared to superconducting coherence length $\xi_{S,N}$.

The rigid SN boundary condition approximation is given formally by the limit $A_S\sigma_S \to \infty$ where there is no inverse proximity effect and the Green's function inside S approaches that of bulk superconductor S′. In the RBC approximation we then consider the Usadel equation with the boundary condition,

$$\hat{g}|_{x=0,L_N} = \hat{g}|_{\mathrm{BCS}}, \quad (11)$$

where the BCS bulk Green's function reads $\hat{g}|_{\mathrm{BCS}} = (\omega_n\tau_3 + \Delta\tau_+ + \Delta^*\tau_-)/\sqrt{\omega_n^2 + |\Delta|^2}$.

For reference, we show in Fig. 1(b) the behavior of the density of states $N(E,x,\varphi)$ at $\varphi = 0$, computed numerically from $\hat{g}$ using the approach outlined in this section without the RBC approximation. The result assumes a non-self-consistent $\Delta(x) = |\Delta|$ in the S regions. Far from the N region ($|x| \gtrsim L_S$), the DOS approaches the BCS form with energy gap $|\Delta|$, whereas towards the N region ($|x| \lesssim L_S$), a minigap E_g [55] becomes clearly visible. Note that, even assuming constant $|\Delta|$, the density of states $N(E,x)$ inside S is modified by the proximity of N.

III. RIGID-BOUNDARY CONDITIONS

According to Eq. (1), supercurrent and entropy are connected by an exact Maxwell relation,

$$\frac{\partial I}{\partial T} = -\frac{2e}{\hbar}\frac{\partial S}{\partial\varphi}. \quad (12)$$

This relation does not hold between Eqs. (2) and (7) within the RBC approximation as one can observe from simple scaling considerations valid in the short-junction regime $L_N \lesssim \xi_N$. Within these approximations, the phase-dependent part of the entropy S is localized in the N region; hence, the volume integral of Eq. (2) scales as $\partial_\varphi S \propto L_N$. In contrast, the supercurrent (8) obtained under the same approximation scales as $\frac{dI}{dT} \propto L_N^{-1}$. Therefore one immediately recognizes that the left- and right-hand sides of Eq. (12) have different dependences on L_N, demonstrating the inconsistency between supercurrent and entropy within these approximations.

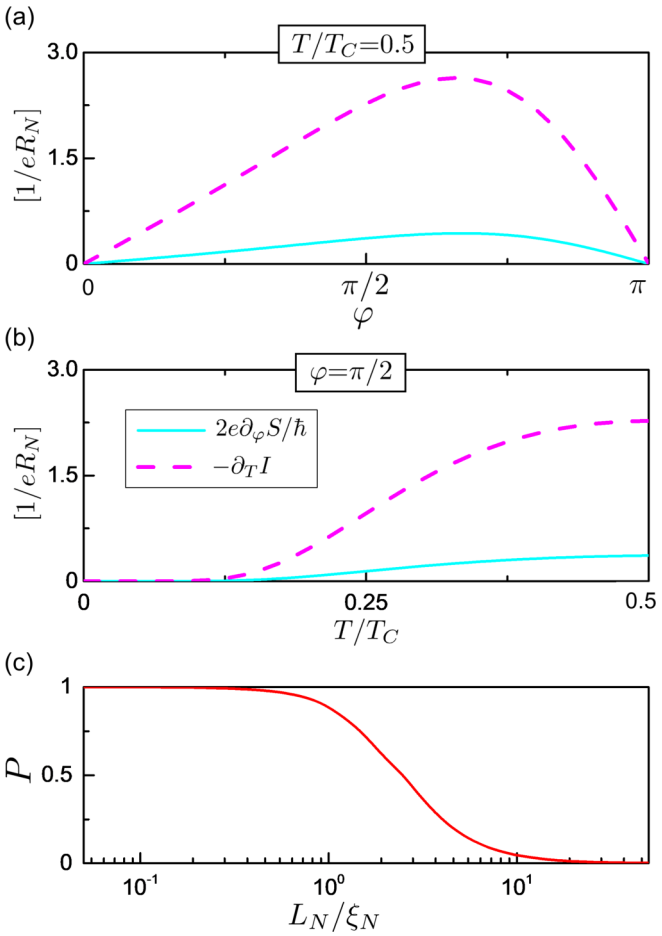

FIG. 2. Inconsistency of the Maxwell relation with the rigid-boundary condition approximation using Eqs. (2) and (7). (a) The left- and right-hand sides of Eq. (12) vs φ at fixed temperature $T = 0.5T_c$ for $\sigma_S A_S = \sigma_N A_N$ and $L_N = \xi_N$. (b) The same vs temperature at $\varphi = \pi/2$. (c) The relative discrepancy P (see the text) as a function of the length of the normal region L_N/ξ_N.

The discrepancy between the DOS expression (2) and the supercurrent (7) evaluated in the RBC approximation extends beyond the short-junction limit as shown in Figs. 2(a) and 2(b). The left- and right-hand sides of Eq. (12) do not match as functions of phase difference φ and temperature T. Figure 2(c) shows the dependence on L_N/ξ_N of the relative discrepancy,

$$P = \max_{(\varphi,T)} \left| \frac{\partial_T I + \frac{2e}{\hbar}\partial_\varphi S}{\partial_T I} \right|. \quad (13)$$

It decreases with increasing junction length L_N and remains significant up to L_N several times the coherence length ξ_N. As one would expect, the discrepancy becomes negligible only for long junctions ($L_N \gg \xi_N$).

Note that in the exact calculation (i.e., without approximations) Eqs. (2) and (7) must be compatible. This is, however, not immediately apparent from the form of the equations. To understand this compatibility we consider now the mathematical relation among Eqs. (2)–(4) [and thus (7)]. Consider a modified Eilenberger functional $\mathcal{L}_\zeta = \mathcal{L}|_{\omega_n \mapsto \omega_n + i\zeta}$ in which the ω_n's appearing explicitly in $\mathcal{L}$ are extended to the complex domain by $\omega_n + i\zeta$ (cf. Ref. [56]) and define the corresponding Green's functions $\hat{g}_\zeta$ satisfying $\delta\mathcal{F}/\delta\hat{g}|_{\hat{g}_\zeta} = 0$ and keep Δ fixed. Recall that the analytic continuation of the sign function is given by $\mathrm{sgn}\, z = z/\sqrt{z^2} = \mathrm{sgn\ Re}\, z$. The stationary value of the functional then satisfies for real ζ,

$$\frac{d}{d\zeta}\mathcal{F}_{s,\zeta}|_{\hat{g}_\zeta,\Delta} = \pi T \mathcal{N}_0 \sum_{\omega_n} \mathrm{tr}[\mathrm{sgn}(\omega_n) - \tau_3 \hat{g}_\zeta(i\omega_n)]$$

$$= -\mathcal{N}_0 \int_{-\infty}^{\infty} dE\,[N_\zeta(E) - 1] \tanh\frac{E}{2T}. \quad (14)$$

The second line follows by standard analytic continuation, where

$N_\zeta(E) = \frac{1}{4}\,\mathrm{tr}\,\tau_3[g_\zeta(E + i0^+) - g_\zeta(E - i0^+)]$. Suppose now that the boundary conditions are *energy independent*, i.e., invariant under transformation $\omega_n \mapsto \omega_n + i\zeta$ of explicit frequency arguments. In this case $\hat{g}_\zeta(i\omega_n) = \hat{g}(i\omega_n - \zeta)$ and $N_\zeta(E) = N(E - \zeta)$ coincide with the energy-shifted Green's function and the corresponding DOS. It is worth noting that $\mathcal{F}_{s,\zeta} \to \mathrm{const}(T)$ for $\zeta \to \infty$ whereas $\hat{g}(i\omega_n - \zeta) \to \tau_3\,\mathrm{sgn}(\omega_n)$. Moreover, recalling the relation,

$$\int_{-\infty}^{0} d\zeta \frac{d}{dT}\tanh\frac{E+\zeta}{2T}$$

$$= -2\{f(E,T)\ln f(E,T) + [1 - f(E,T)]$$

$$\times \ln[1 - f(E,T)]\}, \quad (15)$$

it follows that $\partial_T \mathcal{F}_s = -\mathcal{S}_s$. The Maxwell relation then follows for any fixed Δ independent of T. Finally, setting Δ to its self-consistent value Δ_* for which $\frac{d}{dT}F_s[T,\Delta_*(T)] = \partial_T F_s[T,\Delta_*(T)]$, we find Eqs. (2) and (4) are equivalent—under the assumption that the boundary conditions do not depend on energy.

The boundary value $\hat{g}_{\mathrm{BCS}}(i\omega_n)$ however is strongly energy dependent, which breaks the above argument and causes the discrepancy among Eqs. (2), (4), and (7). It is interesting to note that a similar issue does not occur in an NSN structure under an analogous approximation (also inspected numerically; not shown) because in that case the value of $\hat{g}_N = \tau_3\,\mathrm{sgn}\,\omega_n$ imposed in the boundary condition is invariant under $\omega_n \mapsto \omega_n + i\zeta$. This happens also for insulating interfaces ($\hat{n}\cdot\hat{\nabla}\hat{g} = 0$) or for periodic boundary conditions or semi-infinite leads, which are functionals of $\hat{g}$ with no explicit dependence on ω_n.

The apparent thermodynamic discrepancy can be eliminated by properly taking into account the IP effect, for example, replacing the rigid superconducting boundary condition (11) by S wires of length L_S as depicted in Fig. 1(a). Below, we adopt such a S′SNS S′ geometry with the boundary conditions $\hat{g}|_{x=-L_S} = \hat{g}|_{x=L_N+L_S} = \hat{g}|_{\mathrm{BCS}}$ and consider $L_S \gg \xi_S$. The difference with the exact solution for the semi-infinite leads approaches zero in the limit $L_S \to \infty$.

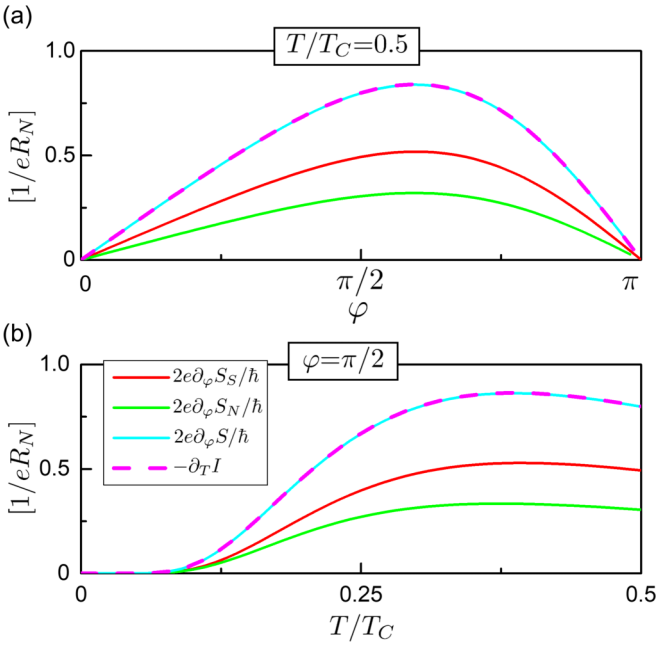

FIG. 3. Maxwell relation including the inverse proximity effect with $L_S = 5\xi_N$. (a) The left- and right-hand sides of Eq. (12) vs φ for $T = 0.5T_c$, $\sigma_S A_S = \sigma_N A_N$, $L_N = \xi_N$. The entropy contributions from the N and S regions $S = S_S + S_N$ also are shown separately. (b) The same vs temperature at $\varphi = \pi/2$.

We show results for such a S′SNS S′ structure in Fig. 3. In them, the Maxwell relation (12) between Eqs. (2) and (4) applies for any L_N. Since we expect the relation applies independently of the form of $\Delta(x)$, this calculation assumes a constant Δ in the leads for simplicity. The phase derivative however is to be understood as in Eq. (7). Finally, note that the entropy contribution from the superconductor regions dominates for the parameters chosen (i.e., relatively short junction).

IV. INVERSE PROXIMITY EFFECT

Let us consider the inverse proximity effect in more detail. We define the entropy difference δS_S due to the inverse proximity effect in the superconducting region as

$$\delta S_S = S_S - S_{\mathrm{BCS}} = -4\int_{-\infty}^{\infty} dE \int_S dx\, \mathcal{N}_{0,S}\delta N$$

$$\times (E,x,\varphi) f(E,T) \ln f(E,T), \quad (16)$$

where S_{BCS} is the entropy of a bulk BCS superconductor and $\delta N(E,x,\varphi) = N(E,x,\varphi) - N_{\mathrm{BCS}}(E)$ is the difference in the local density of states from the BCS expression. Moreover, we define dimensionless parameters,

$$a = \sigma_S A_S/(\sigma_N A_N), \quad l = L_N/\xi_N \quad (17)$$

for the discussion below.

Analytical solutions can be obtained in the limiting cases of short-junction $l \ll 1$ at phase differences $\varphi = 0$ and $\varphi = \pi$. A solution to the Usadel equation in a semi-infinite superconducting wire with uniform $\Delta = \pm|\Delta|$ is

given by

$$\hat{g} = \tau_3 \cosh\theta + i\tau_2 \sinh\theta, \tag{18}$$

where (cf. Ref. [57])

$$\theta(x) = \theta_S - 4\,\mathrm{artanh}\left(e^{-\sqrt{2}(x-L_N)/\xi_E}\tanh\frac{\theta_S-\theta(L_N)}{4}\right), \tag{19}$$

and $\xi_E = (1-E^2/|\Delta|^2)^{-1/4}\xi_N$ and $\theta_S = \mathrm{artanh}\,\frac{|\Delta|}{E+i0^+}$. The spatially integrated change in the superconductor DOS can be evaluated based on this solution,

$$\int_S dx\,\delta N(x,E) = \sqrt{2}\,\mathrm{Re}\left[\xi_E\cosh\theta_S\left(\cosh\frac{\theta_S-\theta(L_N)}{2}-1\right) - \xi_E\sinh\theta_S\sinh\frac{\theta_S-\theta(L_N)}{2}\right]. \tag{20}$$

For $L_N \ll \xi_E$, the Usadel equation in the N region can be approximated as $\partial_x^2\theta(x)=0$. Matching to the boundary condition $\sigma_N A_N \partial_x\theta_N = \sigma_S A_S \partial_x\theta_S$ at the two SN interfaces results in

$$\theta(L_N) = \begin{cases}\theta_S & \text{for } \varphi = 0,\\ \sqrt{2}\frac{\xi_E}{\xi_N} al\,\sinh\frac{\theta_S-\theta(L_N)}{2} & \text{for } \varphi=\pi,\end{cases} \tag{21}$$

from which $\theta(L_N)$ can be solved. For the entropy at $\varphi=0$, this gives a trivial solution $\delta S_S = 0$. On the other hand, at $\varphi=\pi$, we have for temperatures $T \ll |\Delta|$,

$$\delta S_S(\varphi=\pi) \simeq \frac{4\pi^2}{3} T\mathcal{N}_{0,S}A_S\xi_N \times \begin{cases}1 & \text{for } al \ll 1,\\ \frac{\pi}{2al} & \text{for } al \gg 1.\end{cases} \tag{22}$$

The full temperature dependence for $l \to 0$ reads

$$\delta S_S(\varphi=\pi) = -\frac{16}{\sqrt{2}}\mathcal{N}_{0,S}A_S\int_{-\infty}^{\infty} dE\, f(E,T)\ln f(E,T) \times \mathrm{Re}\left[\left(\cosh\frac{\theta_S}{2}-\cosh\theta_S\right)\xi_E\right]. \tag{23}$$

For crossover regions, the boundary condition matching would need to be solved numerically.

The behavior in the RBC limit (i.e., $a\to\infty$) can be understood based on the above result. For the entropy, the short-junction rigid-boundary limit $l\to 0$, $a\to\infty$ is not unique, but the results depend on the product al. Generally, the entropy is proportional to $\hbar/(e^2R_{\mathrm{tot}})$, where R_{tot} is the resistance of the ξ_S-length superconductor segment in series with the normal wire as can be expected *a priori* [26].

Figures 4(a) and 4(b) show the geometry dependence of the proximity effect contribution δS_S to the entropy for $\varphi=0$ and $\varphi=\pi$. Generally, $\delta S_S(\varphi=0)$ decreases with decreasing junction length and approaches the limit of $\delta S_S(\varphi=0)\to 0$ for $l\to 0$. The temperature dependence of $\delta S_S(0)$ is affected largely by the presence of a minigap in the spectrum $S(0)\sim e^{-E_g/T}$ with $E_g \sim \min[\hbar D_N/L_N^2, |\Delta|]$ [see Fig. 1(b)]. For $\varphi=\pi$, on the other hand, the entropy contribution δS_S of the superconductors increases with decreasing length, in accordance with the increase in the Josephson energy with decreasing junction resistance. For very short junctions, $l \lesssim a^{-1}$, δS_S saturates as indicated in Eq. (22). The behavior of $\delta S_S(\varphi=\pi)$ as a function of the product al is shown in Fig. 4(c). It is interesting to note that the results essentially converge to the short-junction limit $l\ll 1$ already at $l=1$.

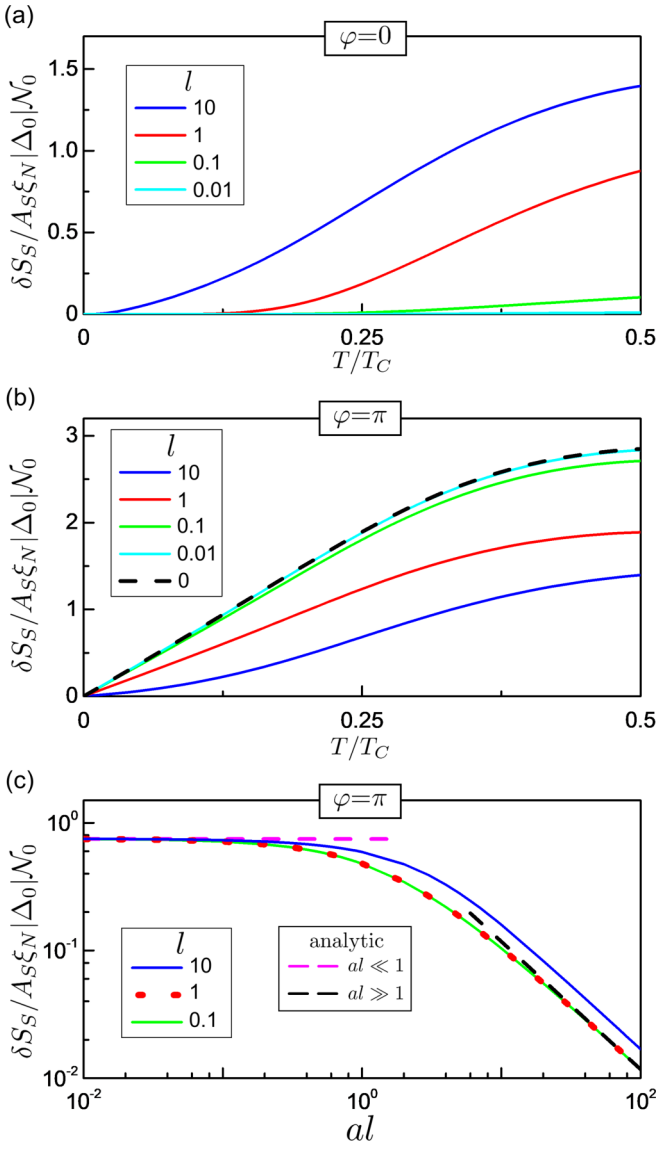

FIG. 4. Behavior of the entropy variation δS_S of the superconducting leads. (a) Temperature dependence at $\varphi=0$ for $a=1$ and different l's. (b) The same at $\varphi=\pi$. Result (23) for $l=0$ also is shown (the dashed line). (c) Dependence of $\delta S_S(\varphi=\pi)$ on l and a at $T/T_C=0.1$. Limiting behavior from Eq. (22) is indicated (the dashed line). Here, $L_S=10\xi_N$.

V. HEAT CAPACITY

The heat capacity,

$$C = T\frac{dS}{dT} \tag{24}$$

can be obtained from the entropy discussed in the previous sections. In Fig. 5 we compare full numerical results obtained

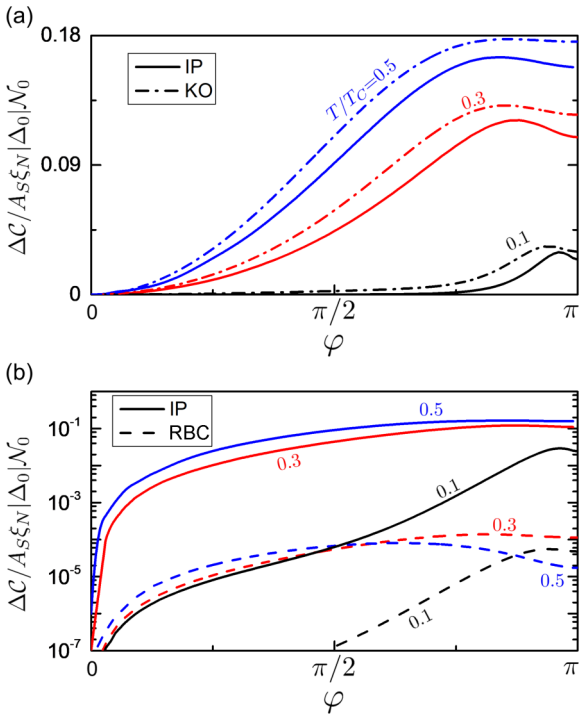

FIG. 5. Modulation of the heat-capacity $\Delta C(T,\varphi) = C(T,\varphi) - C(T,\varphi = 0)$ in a SNS junction for $a = 500$, $l = 0.1$, $L_S = 10\xi_N$. (a) Numerical results comparing the full calculation including the inverse proximity effect (the solid line) with the results from Eq. (9) (KO, the dashed-dotted line) at different temperatures. (b) Comparison between the IP curves from panel (a) and the results from (2) and (11) (RBC, the dashed line) on a logarithmic scale.

from Eqs. (2), (6), and (10) taking the inverse proximity effect into account (the solid lines) with the heat capacity obtained from the KO result (9) (the dashed-dotted lines) and from the numerically computed DOS using the RBC approximation (11) (the dashed lines). In the full numerical calculation, the order parameter $\Delta(x,T)$ is computed to satisfy the self-consistency relations $\delta F/\delta\Delta = \delta F/\delta\Delta^* = 0$. For the selected short-junction lengths $l \ll 1$ and $al \gg 1$, the numerical results obtained by taking the inverse proximity effect into account match relatively well with Eq. (9) weakly overestimating the heat capacity. Note that a self-consistent Δ does not cause significant qualitative deviations. On the other hand, calculations within the RBC approximation using Eq. (2), shown in Fig. 5(b), underestimate the heat capacity by several orders of magnitude. In fact, as pointed out in Sec. III, such an approach is accurate only for long-junctions $L_N \gtrsim 5\xi_N$.

To summarize, although $N(E) - N_{\rm BCS}(E) \to 0$ inside large superconducting banks ($a \to \infty$), the quasiparticle heat-capacity contribution of the proximized S leads: $\delta C \propto a \int dx[N(x,E) - N_{\rm BCS}(x,E)]$ is not negligible. As a consequence, obtaining quasiparticle heat capacity from the DOS requires proper consideration of the inverse proximity effect. The phase dependence of the quasiparticle heat capacity can also be obtained equivalently from the temperature dependence of the super-current-phase relation $I_S(T,\varphi)$. This turns out to be more robust vs neglecting the inverse proximity effect as apparent in Fig. 5(a). However, the heat capacity at $\varphi = 0$ cannot be obtained from this, and it generally will depend on device parameters.

VI. SUMMARY AND DISCUSSION

The entropy in SNS junctions roughly consists of two contributions—a phase-dependent part associated with the bound states contributing also to the supercurrent and a phase-independent part. Generally, the two behave differently as a function of the junction length. Moreover, the phase-dependent contribution in short junctions, if expressed in terms of the local density of states, largely originates from the proximity effect in the superconducting banks. Approximations that neglect this can produce thermodynamically inconsistent results. The results also reiterate as is clear from the connection to the CPR that the junction heat capacity has a part not directly related to the junction volume. A proper quantitative calculation of entropy and thermodynamic quantities taking into account the inverse proximity effect is thus of importance both for fundamental and for application purposes.

Finally, we can consider factors important for an experimental measurement of the heat capacity of a single nanoscale SNS junction. For example, the heat capacity of the junction can be inferred by measuring the temperature variation after a heating pulse as a function of the phase difference, which can be manipulated by means of an external field. For such an experimental realization, two points have to be considered with care. First, the device should be thermally well isolated in order to avoid heat dispersion outside of the device volume itself. Second, the bulk superconductor mass should be made as small as possible. The total heat-capacity C is an extensive property, so its variation as a function of phase difference $\Delta C(\varphi)/C$ increases by increasing the ratio of critical current and device volume. However, this target will also be constrained by the requirement of large superconducting leads in order to ensure the phase bias of the junction, and thus an optimal trade-off has to be considered in a proper device design.

To summarize, we discussed entropy and heat capacity in SNS structures numerically and analytically and point out that inconsistencies appear if inverse proximity contributions are not included properly. The results obtained can be used in designing superconducting devices concerning caloritronic, heat, and photon sensors and are, in general, relevant for other devices based on thermodynamic working principles.

ACKNOWLEDGMENTS

We thank A. Braggio for discussions. P.V., F.V., and F.G. acknowledge funding by the European Research Council under the European Union's Seventh Framework Program (Grant No. FP7/2007-2013)/ERC Grant Agreement No. 615187-COMANCHE and the MIUR under FIRB2013 Grant No. RBFR1379UX-Coca. M.C. acknowledges support from the CNR-CONICET cooperation programme "Energy conversion in quantum, nanoscale, hybrid devices." The work of E.S. was funded by a Marie Curie Individual Fellowship (MSCA-IFEF-ST Grant No. 660532-SuperMag). F.G. acknowledges funding by the Tuscany Region under the FARFAS 2014 Project SCIADRO.

[1] M. Esposito, U. Harbola, and S. Mukamel, Rev. Mod. Phys. **81**, 1665 (2009).

[2] M. Campisi, P. Hänggi, and P. Talkner, Rev. Mod. Phys. **83**, 771 (2011).

[3] F. Giazotto, T. T. Heikkilä, A. Luukanen, A. M. Savin, and J. P. Pekola, Rev. Mod. Phys. **78**, 217 (2006).

[4] M. Carrega, P. Solinas, M. Sassetti, and U. Weiss, Phys. Rev. Lett. **116**, 240403 (2016).

[5] A. Fornieri and F. Giazotto, Towards phase-coherent caloritronics in superconducting circuits, Nat. Nanotechnol. **12**, 944 (2017).

[6] F. Giazotto and M. J. Martínez-Pérez, Nature (London) **492**, 401 (2012).

[7] E. Strambini, F. S. Bergeret, and F. Giazotto, Appl. Phys. Lett. **105**, 082601 (2014).

[8] F. Giazotto and M. J. Martínez-Pérez, Appl. Phys. Lett. **101**, 102601 (2012).

[9] M. J. Martínez-Pérez and F. Giazotto, Appl. Phys. Lett. **102**, 182602 (2013).

[10] A. Fornieri, C. Blanc, R. Bosisio, S. D'Ambrosio, and F. Giazotto, Nat. Nanotechnol. **11**, 258 (2016).

[11] F. Paolucci, G. Marchegiani, E. Strambini, and F. Giazotto, Europhys. Lett. **118**, 68004 (2017).

[12] J. T. Muhonen, M. Meschke, and J. P. Pekola, Rep. Prog. Phys. **75**, 046501 (2012).

[13] P. Solinas, R. Bosisio, and F. Giazotto, Phys. Rev. B **93**, 224521 (2016).

[14] H. Q. Nguyen, J. T. Peltonen, M. Meschke, and J. P. Pekola, Phys. Rev. Appl. **6**, 054011 (2016).

[15] H. Courtois, H. Q. Nguyen, C. B. Winkelmann, and J. P. Pekola, C. R. Phys. **17**, 1139 (2016).

[16] O.-P. Saira, M. Zgirski, K. L. Viisanen, D. S. Golubev, and J. P. Pekola, Phys. Rev. Appl. **6**, 024005 (2016).

[17] A. V. Feshchenko, L. Casparis, I. M. Khaymovich, D. Maradan, O.-P. Saira, M. Palma, M. Meschke, J. P. Pekola, and D. M. Zumbühl, Phys. Rev. Appl. **4**, 034001 (2015).

[18] J. Wei, D. Olaya, B. S. Karasik, S. V. Pereverzev, A. V. Sergeev, and M. E. Gershenson, Nat. Nanotechnol. **3**, 496 (2008).

[19] J. Govenius, R. E. Lake, K. Y. Tan, and M. Möttönen, Phys. Rev. Lett. **117**, 030802 (2016).

[20] A. D. Semenov, G. N. Gol'tsman, and R. Sobolewski, Supercond. Sci. Technol. **15**, R1 (2002).

[21] A. Engel, J. J. Renema, K. Il'in, and A. Semenov, Supercond. Sci. Technol. **28**, 114003 (2015).

[22] J. Voutilainen, M. A. Laakso, and T. T. Heikkilä, J. Appl. Phys. **107**, 064508 (2010).

[23] F. Giazotto, T. T. Heikkilä, G. P. Pepe, P. Helistö, A. Luukanen, and J. P. Pekola, Appl. Phys. Lett. **92**, 162507 (2008).

[24] J. Govenius, R. E. Lake, K. Y. Tan, V. Pietilä, J. K. Julin, I. J. Maasilta, P. Virtanen, and M. Möttönen, Phys. Rev. B **90**, 064505 (2014).

[25] B. S. Karasik, S. V. Pereverzev, A. Soibel, D. F. Santavicca, D. E. Prober, D. Olaya, and M. E. Gershenson, Appl. Phys. Lett. **101**, 052601 (2012).

[26] K. K. Likharev, Rev. Mod. Phys. **51**, 101 (1979).

[27] B. Pannetier and H. Courtois, J. Low Temp. Phys. **118**, 599 (2000).

[28] J. Bardeen, L. N. Cooper, and J. R. Schrieffer, Phys. Rev. **108**, 1175 (1957).

[29] L. P. Gor'kov, Zh. Eksp. Teor. Fiz. **36**, 1918 (1959) [Sov. Phys. JETP **9**, 1364 (1959)].

[30] G. Eilenberger, Z. Phys. **214**, 195 (1968).

[31] A. A. Golubov, M. Y. Kupriyanov, and E. Il'ichev, Rev. Mod. Phys. **76**, 411 (2004).

[32] C. W. J. Beenakker and H. van Houten, in *Nanostructures and Mesoscopic Systems: Proceedings of the International Symposium, Santa Fe, 1991*, edited by W. P. Kirk and M. A. Reed (Academic, San Diego, 1991).

[33] C. W. J. Beenakker and H. van Houten, Phys. Rev. Lett. **66**, 3056 (1991).

[34] I. Kosztin, Š. Kos, M. Stone, and A. J. Leggett, Phys. Rev. B **58**, 9365 (1998).

[35] S. Kos and M. Stone, Phys. Rev. B **59**, 9545 (1999).

[36] P. Fulde and W. Moormann, Phys. kondens. Mater. **6**, 403 (1967).

[37] M. P. Zaitlin, Phys. Rev. B **25**, 5729 (1982).

[38] R. L. Kobes and J. P. Whitehead, Phys. Rev. B **38**, 11268 (1988).

[39] C.-R. Hu, Phys. Rev. B **6**, 1 (1972).

[40] G. Eilenberger and A. E. Jacobs, J. Low Temp. Phys. **20**, 479 (1975).

[41] J. A. Blackburn, B. B. Schwartz, and A. Baratoff, J. Low Temp. Phys. **20**, 523 (1975).

[42] J. Lechevet, J. E. Neighbor, and C. A. Shiffman, Phys. Rev. B **5**, 861 (1972).

[43] P. Manuel and J. J. Veyssié, Phys. Rev. B **14**, 78 (1976).

[44] M. Y. Kupriyanov and V. F. Lukichev, Fiz. Nizk. Temp. **8**, 1045 (1982).

[45] H. Rabani, F. Taddei, O. Bourgeois, R. Fazio, and F. Giazotto, Phys. Rev. B **78**, 012503 (2008).

[46] H. Rabani, F. Taddei, F. Giazotto, and R. Fazio, J. Appl. Phys. **105**, 093904 (2009).

[47] K. D. Usadel, Phys. Rev. Lett. **25**, 507 (1970).

[48] A. Altland, B. D. Simons, and D. Taras-Semchuk, Pis'ma Zh. Eksp. Teor. Fiz. **67**, 21 (1998) [JETP Lett. **67**, 22 (1998)].

[49] D. Taras-Semchuk and A. Altland, Phys. Rev. B **64**, 014512 (2001).

[50] A. Levy Yeyati, A. Martín-Rodero, and F. J. García-Vidal, Phys. Rev. B **51**, 3743 (1995).

[51] As usual, the complex conjugate is formally a separate variable in the derivative.

[52] I. O. Kulik and A. N. Omel'yanchuk, Pis'ma Zh. Eksp. Teor. Fiz. **21**, 216 (1975) [JETP. Lett. **21**, 96 (1975)].

[53] M. Y. Kupriyanov and V. F. Lukichev, Zh. Eksp. Teor. Fiz. **94**, 139 (1988) [Sov. Phys. JETP **67**, 1163 (1988)].

[54] Y. V. Nazarov, Phys. Rev. Lett. **73**, 1420 (1994).

[55] F. Zhou, P. Charlat, B. Spivak, and B. Pannetier, J. Low Temp. Phys. **110**, 841 (1998).

[56] H. Burkhardt and D. Rainer, Ann. Phys. (N.Y.) **506**, 181 (1994).

[57] A. D. Zaikin and G. F. Zharkov, Fiz. Nizk. Temp. **7**, 375 (1981) [J. Low Temp. Phys. **7**, 184 (1981)].